American Mineralogist, Volume 75, pages 247–255, 1990

An EXAFS study of thiospinel minerals

J. Charnock, C. D. Garner
Department of Chemistry, The University, Manchester M13 9PL, England
R.A.D. Pattrick, D. J. Vaughan
Department of Geology, The University, Manchester M13 9PL, England

Abstract

The technique of extended X-ray absorption fine structure (EXAFS) spectroscopy has been employed to study certain thiospinel minerals. The EXAFS spectra (and associated Fourier transforms of the spectra) of Cu and Co in end-member carrollite ($CuCo_2S_4$) and of Fe and Cr in daubréelite ($FeCr_2S_4$) are reported, along with corresponding data for Fe and Ni in a series of "violarites" of compositions $Fe_{0.25}Ni_{2.75}S_4$, $Fe_{0.75}Ni_{2.25}S_4$, and $FeNi_2S_4$. The spectra provide direct evidence that daubréelite is a normal spinel and that carrollite contains Cu wholly within the tetrahedral sites. Discrepancies between the EXAFS parameters and previously reported crystallographic data for carrollite could be associated with local distortions of the octahedral site. The EXAFS data for the violarites provide clear evidence that in the series Ni_3S_4-$FeNi_2S_4$, Fe substitutes for Ni in the octahedral sites, in agreement with predictions made on the basis of previously published crystal-chemical models.

Introduction

The thiospinels (or sulfospinels) are a group of metal sulfides with the spinel crystal structure. Synthetic thiospinels form a large group of solids with interesting electrical and magnetic properties (Von Philipsborn, 1974); the mineral thiospinels (M_3S_4 phases, where M can be Fe, Co, Ni, Cu, Cr, In, and possibly Pt), although much fewer in number, form a diverse group of phases that exemplify problems of more general interest in sulfide mineralogy (Vaughan and Craig, 1978). Mineral thiospinels, named according to ideal end-member compositions, exhibit extensive solid solutions based on the series carrollite ($CuCo_2S_4$)–linnaeite (Co_3S_4)–polydymite (Ni_3S_4)–violarite ($FeNi_2S_4$). Other members of the thiospinel group, notably daubréelite ($FeCr_2S_4$), greigite (Fe_3S_4), and the rare mineral indite ($FeIn_2S_4$), generally occur as relative pure end-members.

Data on the properties, phase relations, and crystal chemistry of the thiospinel minerals are provided by Vaughan et al. (1971) and Vaughan and Craig (1978), whereas the systematics of the spinel structure-type have been reviewed by Hill et al. (1979). Although the minerals of this group have the familiar spinel crystal structure, which is based on cubic closest-packing of S with half the octahedral sites and one-eighth of the tetrahedral sites occupied by cations (Lundqvist, 1947) and hence one tetrahedral (A) cation site and two octahedral (B) cation sites per formula unit (AB_2S_4), there has been disagreement over the precise symmetry and structure of these and other spinel phases. Like the oxide spinels, thiospinels have normally been referred to the space group $Fd3m$, but Grimes (1972) has suggested that the space group $F\bar{4}3m$ may be more appropriate to many of these compounds. This assignment is consistent with evidence that the octahedrally coordinated metal ions may be "off-center" and displaced along [111] directions, evidence that is particularly strong for the oxide spinels $MgAl_2O_4$ (Grimes et al., 1983) and Fe_3O_4 (Collyer et al., 1988). For the thiospinels, Higgins et al. (1975) found evidence from X-ray diffraction that carrollite, linnaeite, and siegenite possess a symmetry lower than $Fd3m$ but consistent with several other cubic space groups, including $F\bar{4}3m$. Grimes (1974), on the other hand, examined power-diffraction data and found only a slight improvement in fitting of the data when the space group $F\bar{4}3m$ was applied to $CuCo_2S_4$, whereas for many oxide spinels the improvement was appreciable. However, other studies have found that cation ordering on octahedral sites in $Fe_{0.76}Yb_{2.16}S_4$ (Tomas and Guittard, 1977) and on tetrahedral sites in $FeIn_2S_4$ (Hill et al., 1979) reduces those spinels to $F\bar{4}3m$ symmetry. Clearly, some uncertainties remain as to the precise structure of the thiospinels, but some evidence at least supports a structure with a symmetry lower than $Fd3m$.

Another aspect of spinel crystal chemistry concerns the occupancy of divalent and trivalent cations in tetrahedral and octahedral sites giving normal and inverse spinel types. Although the assignment of formal oxidation states in oxide spinels categorized as normal (e.g., $Mg^{2+}Al_2^{3+}O_4$) or inverse (e.g., $Fe^{3+}(Mg^{2+}Fe^{3+})O_4$) may be relatively straightforward, the situation in the thiospinels is more complex because of the effects of electron delocalization (Vaughan et al., 1971). The questions regarding formal oxidation states are inevitably concerned with the electronic structures of the thiospinels, which have been dis-

0003–0004X/90/0304–0247$02.00

cussed on the basis of qualitative models by Vaughan et al. (1971) and further developed on the basis of quantum chemical calculations by Vaughan and Tossell (1981). Such electronic-structure models have been developed with regard to the observed structural, electrical, and magnetic properties of the thiospinels alongside theoretical considerations.

The technique of extended X-ray absorption fine structure (EXAFS) spectroscopy has not previously been systematically applied to the thiospinel minerals. It is capable of determining the occupancy of cations of a particular oxidation state in particular sites in a mineral, as well as providing site-specific information on bond lengths and other useful crystal chemical data. In the present work, carefully characterized natural samples of the end-member thiospinel minerals daubréelite ($FeCr_2S_4$) and carrollite ($CuCo_2S_4$) have been examined along with a series of three synthetic "violarite" samples of compositions, $FeNi_2S_4$, $Fe_{0.75}Ni_{2.25}S_4$, and $Fe_{0.25}Ni_{2.75}S_4$. Electron-probe microanalysis confirms that the daubréelite and carrollite are pure end-members, and their cell parameters are consistent with the values given by Vaughan et al. (1971) for such compositions. The violarite samples are members of a series previously studied using ^{57}Fe Mössbauer spectroscopy, and details of their synthesis and characterization (including cell parameters) are given in Vaughan and Craig (1985).

Experimental methods

Samples were finely ground under acetone and pressed into Al sample holders with Scotch-tape windows. The EXAFS spectra were collected at room temperature in transmission mode on station 7.1 at the Daresbury Synchrotron Radiation Source, operating at 2 GeV with an average current of 150 mA. A Si(111) double-crystal monochromator was used with the crystal faces offset to give 50% rejection of the beam in order to reduce harmonic contamination. Ion chambers to detect the incident and transmitted radiation were filled with Ar-He mixtures to absorb 20% and 80% of the beam, respectively. The samples were diluted with boron nitride to give absorption just before the edge of about zero, and an increment in the absorption at the edge of approximately 1.0, where possible. For samples with a high background absorption, such as the Fe spectrum of $Fe_{0.25}Ni_{2.75}S_4$ violarite, the edge step was lower and multiple scans were taken and averaged to improve the signal-to-noise ratio. Otherwise, a single scan was considered to give data having a satisfactory signal-to-noise ratio.

Data analysis utilized the single-scattering spherical-wave method for calculating EXAFS (Lee and Pendry, 1975) with phase shifts derived from ab initio calculations, using the Daresbury program EXCURVE (Gurman et al., 1984), the relaxed 1*s* core-hole approximation for the central atom, and the program default parameters for the muffin tin radii, ionic charge, and exchange terms. The phase shifts were not further refined using spectra of model compounds. A fit was produced by generating a theoretical spectrum from a structure of several shells of backscatterers around the central atom, and allowing parameters defining bond lengths and Debye-Waller factors in each shell to vary iteratively to give the best agreement with the experimental data. For the violarite samples the coordination numbers were also iterated in order to detect any changes. Only those shells that made a significant improvement to the fit were included in the simulations.

Results

Figures 1 and 2 show the EXAFS spectra and associated Fourier transforms of the Co and Cu in carrollite and of the Cr and Fe in daubréelite, and the quality of the fit between experimental and simulated data. The Fourier transforms of the spectra represent approximate radial distribution functions around the central atoms, with each peak corresponding to a shell (or groups of closely spaced shells) of backscattering atoms. However, in certain cases, destructive interference among the EXAFS contributions from different shells may lead to a significant diminution in the intensity of the peaks in both the EXAFS and Fourier transform. The EXAFS and their Fourier transforms for these metal atoms divide into two groups, Co in carrollite and Cr in daubréelite on the one hand and Cu in carrollite and Fe in daubréelite on the other. The X-ray crystallographic data available for these minerals (De Jong and Hoog, 1928; Lundqvist, 1943) indicate that both are normal spinels, with Co and Cr in octahedral sites and Cu and Fe in tetrahedral sites. These conclusions are consistent with the EXAFS data. Thus, for each pair (Co vs. Cu; Cr vs. Fe), the amplitude of the first shell of backscattering atoms (S) in the Fourier transform (Fig. 2) is 20–30% higher for the former as compared to the latter element. Furthermore, the profiles of the radial distribution curves provide a clear fingerprint of each site, with the relative position of the backscattering contributions being that expected from the crystal structure. Thus (using the numerical data obtained from interpretation of the EXAFS, Tables 1 and 2), for octahedral sites with $M - S = a$, the second and third shells are distinct and manifest at ca. $1.5a$ and $1.75a$, with other contributions being relatively weak but apparent in the appropriate regions in the Fourier transforms. The second shell consists of 6 M^{3+} (Co or Cr) atoms and the third shell of 6 M^{2+} (Cu or Fe) atoms. For the Co spectrum in carrollite, the fit is improved by including the shell of 12 Co backscatterers at 5.79 Å ($2.3a$). For tetrahedral sites, with $M - S = b$, the second (12 M^{3+} = Co or Cr) and third (12 S) shells are not resolved in the Fourier transform and appear at $1.70–1.75b$, with other prominent contributions arising from 16 M^{3+} (Co or Cr) atoms at $2.8b$. These results demonstrate that the octahedral site in thiospinels can be clearly distinguished from the tetrahedral site by the nature of the EXAFS and its Fourier transform. In contrast, the X-ray absorption near-edge structure (XANES) region of the X-ray absorption spectra (Fig. 3) shows no clear correlation with the nature of the site.

The parameters derived from the interpretation of the

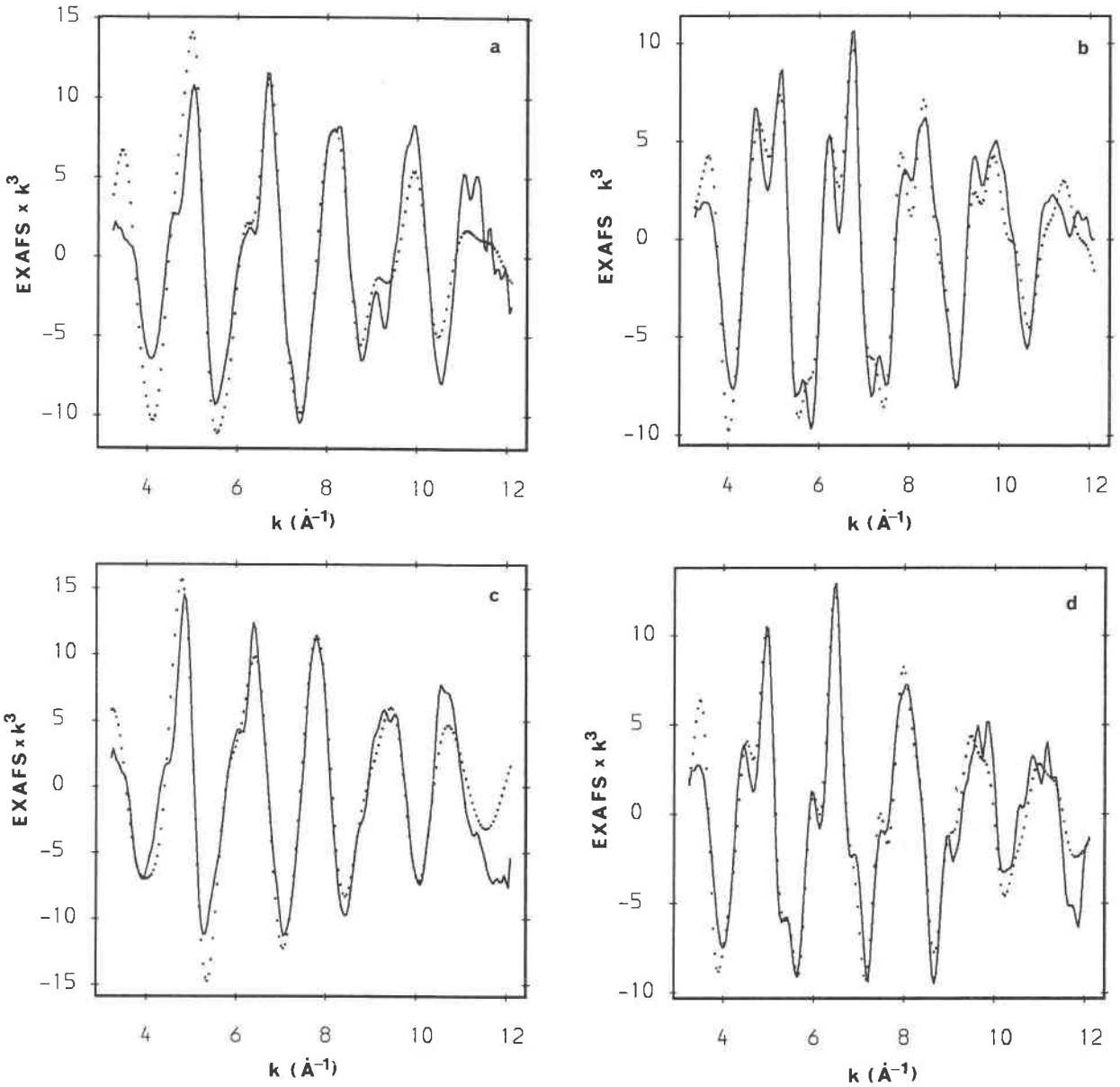

Fig. 1. The k^3-weighted EXAFS spectra of carrollite, (**a**) Co EXAFS and (**b**) Cu EXAFS, and of daubréelite, (**c**) Cr EXAFS and (**d**) Fe EXAFS (solid lines, experimental data; dots, simulated data).

EXAFS data are presented in Tables 1 and 2, where they are compared with the corresponding dimensions obtained from X-ray crystallographic studies. We consider that the information obtained from these EXAFS studies is a more realistic description of the coordination environments of the cations, especially in respect to the distances obtained, than the earlier crystallographic studies. These latter studies were accomplished during the early days of X-ray crystallography and may therefore involve significant errors in the values obtained. This uncertainty is especially important for carrollite, in relation to which problems concerning the precise structure are discussed below.

The EXAFS spectra and Fourier transforms of the Fe and Ni in the three violarite samples are shown in Figures 4, 5, and 6, and the best-fit theoretical parameters are presented in Tables 3 and 4. Although analysis of EXAFS data generally leads to errors of ca. ±25% in the absolute values of coordination numbers, particularly when uncalibrated (i.e., unreferenced to a standard model compound) phase shifts are used (as is the case here), the relative values obtained should reflect differences in coordination numbers among samples. As the Fe content increases from 0.25 to 1.0 atoms per formula unit, it can be seen that the EXAFS spectra and Fourier transforms do not change significantly, and there is little variation in the

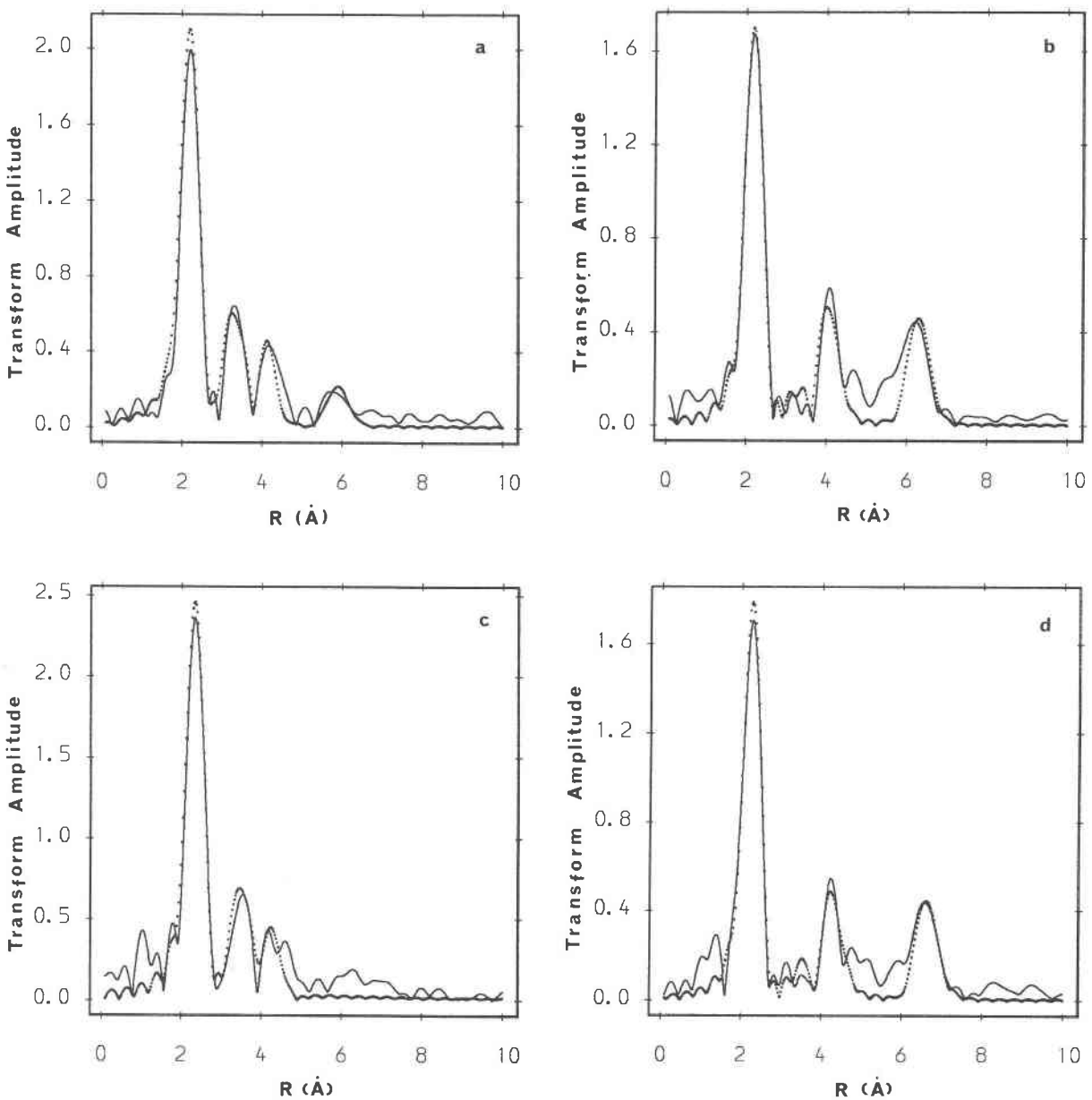

Fig. 2. Fourier transforms of the EXAFS spectra of carrollite, (**a**) Co EXAFS and (**b**) Cu EXAFS, and of daubréelite, (**c**) Cr EXAFS and (**d**) Fe EXAFS (solid lines, experimental data; dots, simulated data).

best-fit parameters, especially for the first and third shells. The change in the apparent coordination number in the second shell is probably due to changes in the backscatterers contributing to that shell. As can be seen from the crystal structures of carrollite and daubréelite, the shell of atoms at ca. 3.5 Å that surrounds the octahedral site is made up of other octahedrally coordinated atoms. In $Fe_{0.25}Ni_{2.75}S_4$, most of the metal atoms in both tetrahedral and octahedral sites are Ni. However, if the Fe content increases and if Fe orders on one site, then backscattering from that site will include contributions from both Fe and Ni. These may tend to cancel out, especially if their distances from the central atom are slightly different. Attempts to simulate this second shell showed that a good fit would be obtained from a wide range of parameter values, and in particular the occupation numbers for the Fe and Ni backscatterers were very ill defined. Therefore, we have not based our conclusions on the interpretation of this shell. However, this problem should not affect the first shell, in which all of the backscatterers are S atoms. From Table 3 it can be seen that all three Fe spectra yield very similar first shell parameters, which implies that the Fe occupies the same site (or sites) in all three samples. The XANES regions of the Fe and the Ni spectra show only

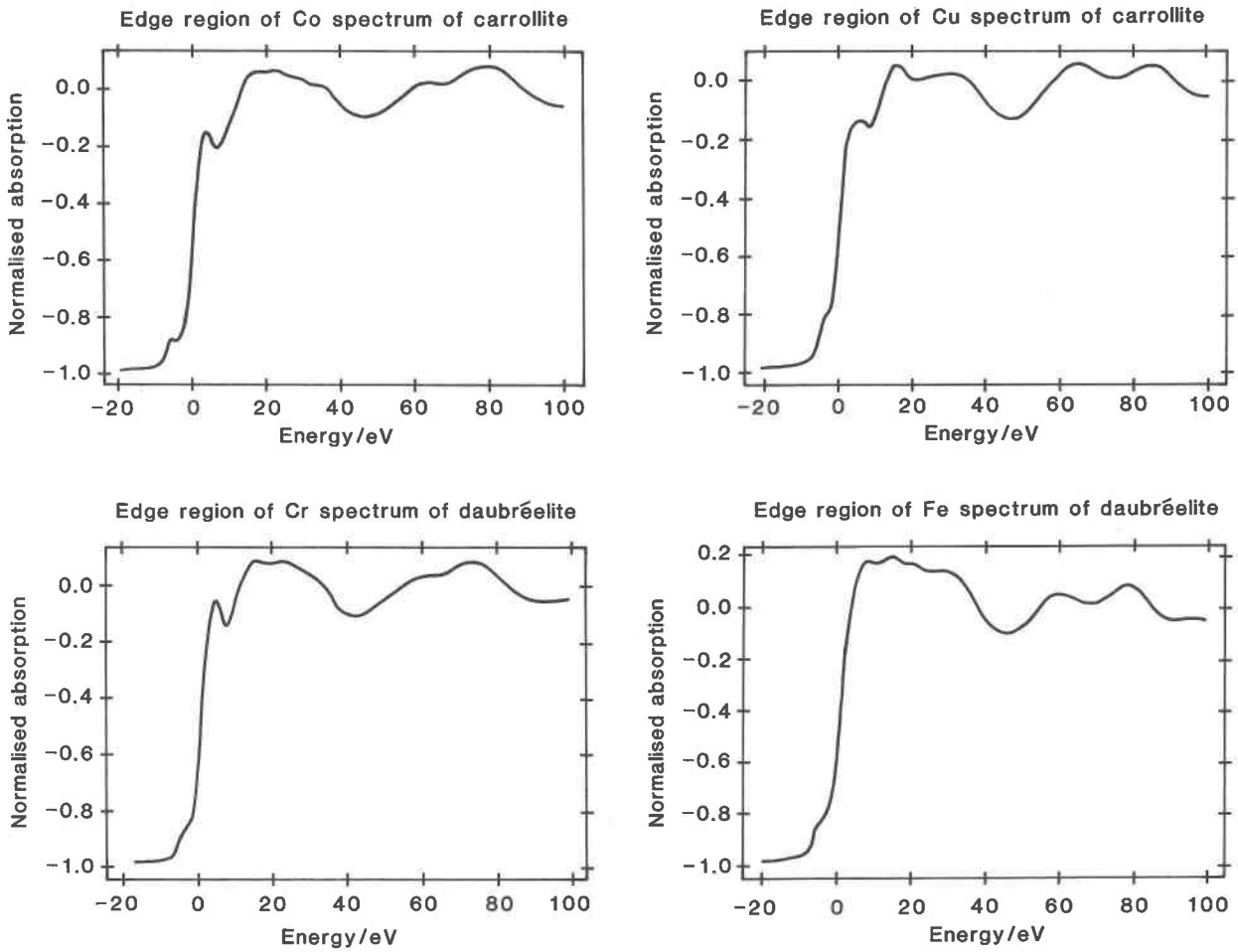

Fig. 3. X-ray absorption spectra in the edge regions for Co and Cu in carrollite and Cr and Fe in daubréelite.

Table 1. Comparison of EXAFS and X-ray–crystallographic parameters for carrollite

Central atom	Shell	X-ray crystallography distance (Å)*	EXAFS†	
			R (Å)‡	$2\sigma^2$ (Å²)§
Co	6 × S	2.365	2.24	0.015
	6 × Co	3.344	3.33	0.025
	6 × Cu	3.921	3.94	0.025
	8 × S	4.095		
	24 × S	5.287		
	12 × Co	5.792	5.79	0.044
Cu	4 × S	2.048	2.22	0.013
	12 × S	3.921	3.79	0.041
	12 × Co	3.921	3.84	0.031
	4 × Cu	4.095		
	12 × S	5.153		
	12 × S	6.143		
	16 × Co	6.143	6.23	0.026

* Error could be large, as the work was accomplished during the early days of X-ray crystallography and no esd's were given.
† Only the major shells contributing to the EXAFS were included in the fit.
‡ Distance ±0.02 Å (first shell), ±0.05 Å (outer shells).
§ Debye-Waller factor.

Table 2. Comparison of EXAFS and X-ray–crystallographic parameters in daubréelite

Central atom	Shell	X-ray crystallography distance (Å)	EXAFS†	
			R (Å)‡	$2\sigma^2$ (Å²)§
Cr	6 × S	2.462	2.37	0.011
	6 × Cr	3.524	3.50	0.024
	6 × Fe	4.132	4.12	0.030
	2 × S	4.264		
	6 × S	4.333		
	12 × S	5.558		
	12 × S	5.611		
	12 × Cr	6.103		
Fe	4 × S	2.209	2.30	0.011
	12 × S	4.141	3.93	0.046
	12 × Cr	4.132	4.04	0.033
	4 × Fe	4.315		
	12 × S	5.396		
	12 × S	6.433		
	16 × Cr	6.473	6.56	0.026

† Only the major shells contributing to the EXAFS were included in the fit.
‡ Distance ±0.02 Å (first shell), ±0.05 Å (outer shells).
§ Debye-Waller factor.

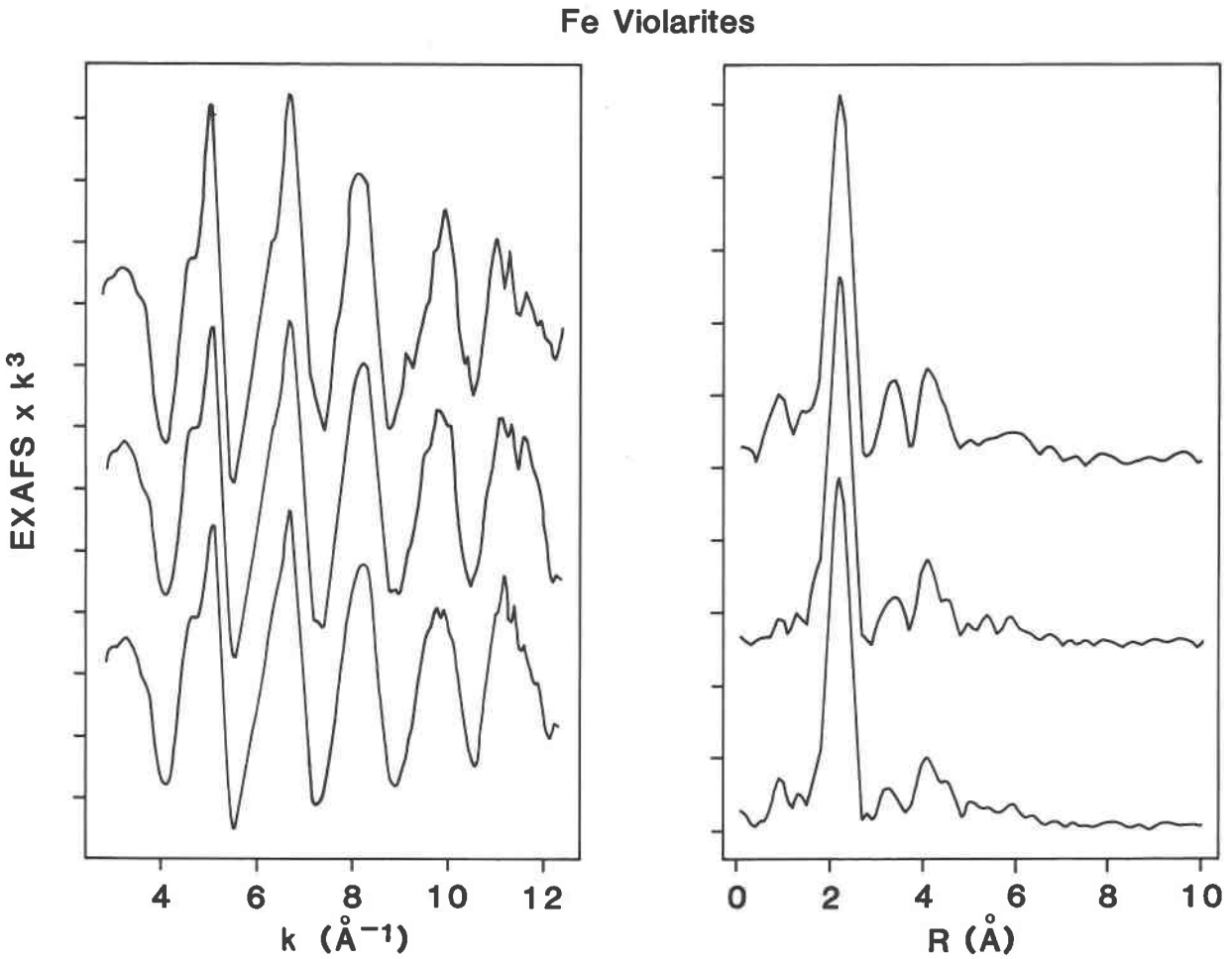

Fig. 4. The k^3-weighted Fe EXAFS spectra of the three violarite samples of composition $Fe_{0.25}Ni_{2.75}S_4$ (top), $Fe_{0.75}Ni_{2.25}S_4$ (middle), and $FeNi_2S_4$ (bottom) shown on the left side, with Fourier transforms of each shown on the right side.

very minor changes among the samples. The edge shifts of the three Fe spectra are 7.0 ± 0.2 eV with respect to metallic Fe, and the Ni edge shifts are 5.3 ± 0.2 eV with respect to metallic Ni. The presence of a peak at 3.2 Å in the Fourier transform and the absence of a peak at ca. 6.1–6.5 Å shows that most or all of the Fe must be in octahedral coordination. The Ni spectra and Fourier transforms do change slightly as the Ni content decreases.

All three spectra exhibit features characteristic of a combination of octahedral and tetrahedral coordination, with peaks in the Fourier transforms at both 3.2 and 6.1 Å. As the Fe content increases, the peak at 3.2 Å, a feature of octahedral coordination, decreases in intensity, and the peak at 6.1 Å, which arises from tetrahedral coordination, increases slightly. However, these features will be affected by changes in the nature of the backscatterers, as some of the Ni is replaced by Fe, and so such features do not give an unequivocal picture of which sites remain occupied by Ni. Changes in the first shell, which consists of S backscatterers, give a more reliable guide to changes in the Ni environment, and since EXAFS measures the average coordination environment of all the Ni atoms in each sample, these changes in parameters reflect changes in the distribution of Ni between the two sites. With increasing Fe content, the observed Ni-S bond length and Ni coordination number both decrease. A higher coordination number and longer bond length would be associated with the octahedral site, so that the Ni in the sample of composition $Fe_{0.25}Ni_{2.75}S_4$ shows more octahedral character than in sample $Fe_{0.75}Ni_{2.25}S_4$, which in turn is more octahedral in character than sample $Fe_1Ni_2S_4$. These results suggest that the Fe is tending to replace the Ni in octahedral rather than tetrahedral sites.

Discussion

The EXAFS spectra of the thiospinels provide direct evidence that $FeCr_2S_4$ is a normal spinel (i.e., in terms of formal oxidation states a species that may be described as $([^4]Fe^{2+}[^6]Cr_2^{3+}S_4)$ in agreement with the evidence provided by Mössbauer spectroscopy (Greenwood and Whitfield, 1968) and expected on the basis of crystal-chemical models (Vaughan et al., 1971). The spectra also provide

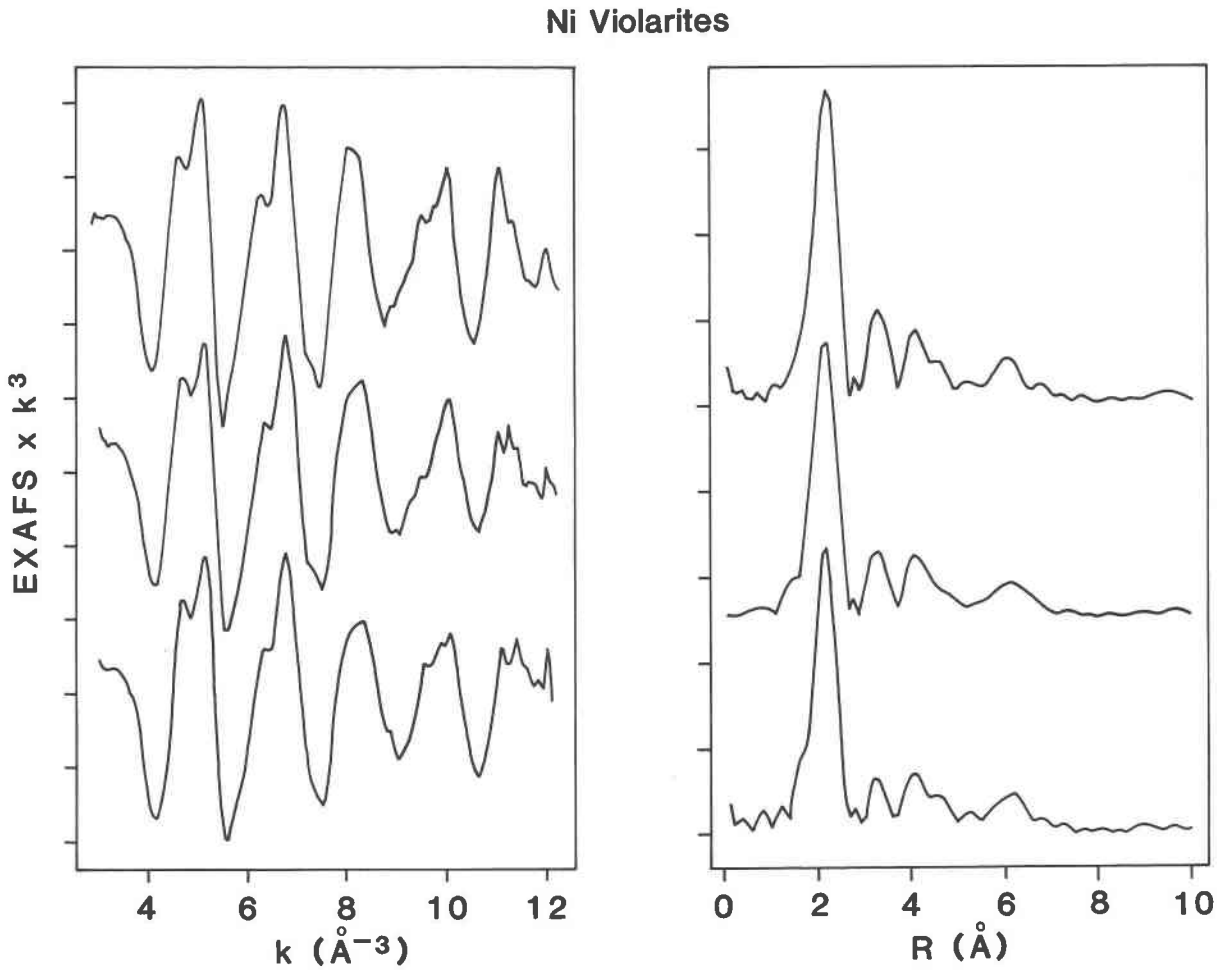

Fig. 5. The k^3-weighted Ni EXAFS spectra of the three violarite samples of compositions $Fe_{0.25}Ni_{2.75}S_4$ (top), $Fe_{0.75}Ni_{2.25}S_4$ (middle), and $FeNi_2S_4$ (bottom) shown on the left side, with Fourier transforms of each shown on the right side.

direct evidence that carrollite is a spinel in which Cu is contained wholly within the tetrahedral sites. Again, the assignment of formal oxidation states would lead to the identification of carrollite as a normal spinel ($^{[4]}Cu^{2+}{}^{[6]}Co_2^{3+}S_4$) although, in this case, the metallic properties imply that the use of formal oxidation states may be misleading.

The discrepancies between EXAFS parameters and crys-

TABLE 3. EXAFS parameters from the Fe spectra of violarite

Sample	Back-scatterer	N*	R (Å)†	$2\sigma^2$ (Å²)‡
$Fe_{0.25}$	S	4.9	2.26	0.012
	Ni	2.3	3.32	0.015
	Ni	5.8	3.93	0.025
$Fe_{0.75}$	S	4.7	2.25	0.012
	Ni	1.8	3.32	0.019
	Ni	4.5	3.90	0.024
$Fe_{1.0}$	S	4.7	2.26	0.013
	Ni	0.9	3.32	0.013
	Ni	5.1	3.90	0.028

* Coordination number ±25% (first shell).
† Distance ±0.02 Å (first shell), ±0.05 Å (outer shell).
‡ Debye-Waller factor.

TABLE 4. EXAFS parameters from the Ni spectra of violarite

Sample	Back-scatterer	N*	R (Å)†	$2\sigma^2$ (Å²)‡
$Fe_{0.25}$	S	4.2	2.25	0.016
	Ni	1.0	3.32	0.007
	Ni	4.0	3.87	0.029
	Ni	8.5	6.24	0.035
$Fe_{0.75}$	S	3.7	2.23	0.016
	Ni	0.9	3.29	0.010
	Ni	2.4	3.84	0.024
	Ni	9.1	6.18	0.037
$Fe_{1.0}$	S	3.6	2.22	0.015
	Ni	0.6	3.30	0.008
	Ni	1.8	3.83	0.018
	Ni	9.2	6.17	0.035

* Coordination number ±25% (first shell).
† Distance ±0.02 Å (first shell), ±0.05 Å (outer shell).
‡ Debye-Waller factor.

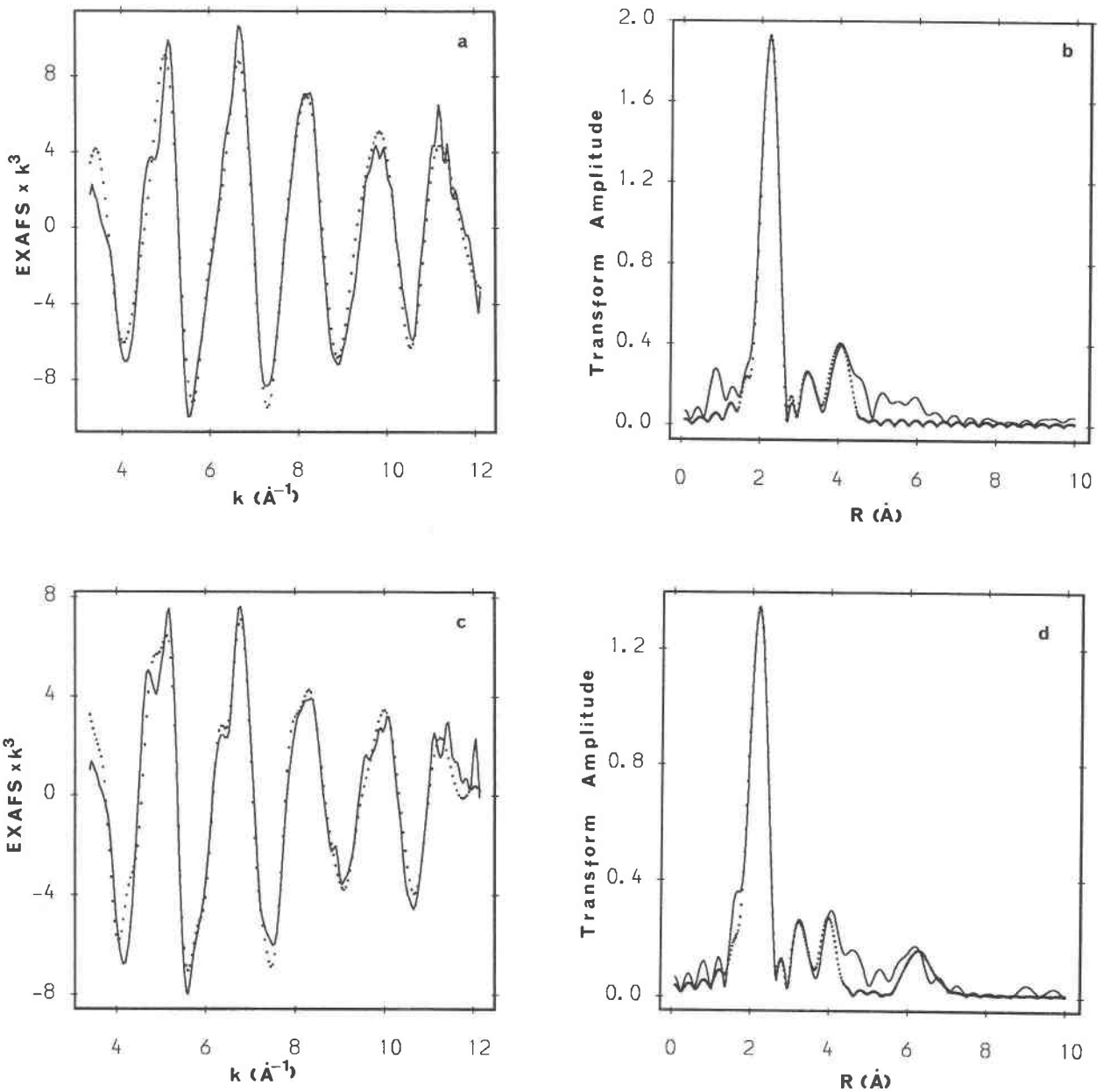

Fig. 6. The k^3-weighted Fe and Ni EXAFS spectra of violarite ($FeNi_2S_4$), (**a**) Fe EXAFS and (**c**) Ni EXAFS, and the Fourier transforms of these spectra, (**b**) Fe EXAFS and (**d**) Ni EXAFS (solid lines, experimental data; dots, simulated data).

tallographic parameters for carrollite referred to above could perhaps be explained by local distortions associated with a noncentrosymmetric space group (e.g., $F\bar{4}3m$) as indicated by certain of the detailed X-ray studies of this phase (e.g., Higgins et al., 1975). Although the EXAFS data are not direct evidence of local distortions of the type envisaged in producing the noncentrosymmetric structure, it is further support for these theories.

The EXAFS data for the violarites discussed above are particularly interesting. In this case, crystal-chemical models aimed at explaining the metallic conductivity, magnetic properties, unit-cell parameters, extent of solid solution with the Ni_3S_4 end-member, and such mineralogical properties as reflectance and microhardness require that the Fe substituting for Ni in the series Ni_3S_4-$FeNi_2S_4$ does so in the octahedral sites (Vaughan et al., 1971). Although attempts to refine models by using the results of molecular orbital calculations (Vaughan and Tossell, 1981) and studies of the ^{57}Fe Mössbauer spectra (Vaughan and Craig, 1985) have lent further support to these theories, the EXAFS data reported here provide the most conclusive evidence so far obtained.

Acknowledgments

We thank the SERC for financial support and the Director of the Daresbury Laboratory for provision of facilities.

References cited

Collyer, S., Grimes, N.W., and Vaughan, D.J. (1988) Does magnetite lack a centre of symmetry? Journal of Physics C (Solid State Physics), 21, L989–L992.

De Jong, W.F., and Hoog, A. (1928) Carrollite (sychnodymite). Zeitschrift für Kristallographie, 66, 168–171.

Greenwood, N.N., and Whitfield, H.J. (1968) Mössbauer effect studies on cubanite ($CuFe_2S_3$) and related iron sulfides. Journal of the Chemical Society, A, 1697–1699.

Grimes, N.W. (1972) "Off centre" ions in compounds with spinel structure. Philosophical Magazine, 26, 1217–1226.

——— (1974) An X-ray diffraction investigation of sulfide spinels. Journal of Physics D: Applied Physics, 7, 1–6.

Grimes, N.W., Thompson, P., and Kay, H.F. (1983) New symmetry and structure for spinel. Proceedings of the Royal Society, A386, 333–345.

Gurman, S.J., Binstead, N., and Ross, I. (1984) A rapid exact curved-wave theory for EXAFS calculations. Journal of Physics, C17, 143–151.

Higgins, J.B., Speer, J.A., and Craig, J.R. (1975) A note on thiospinel space group assignment. Philosophical Magazine, 32, 685.

Hill, R.J., Craig, J.R., and Gibbs, G.V. (1979) Systematics of the spinel structure type. Physics and Chemistry of Minerals, 4, 317–339.

Lee, P.A., and Pendry, J.B. (1975) Theory of extended X-ray absorption fine structure. Physical Review, B11, 2795–2811.

Lundqvist, D. (1943) Crystal structure of daubréelite. Arkiv för Kemi Mineralogi och Geologi, 17B, no. 12, 4 p.

——— (1947) X-ray studies on the ternary system Fe-Ni-S. Arkiv för Kemi Mineralogi och Geologi, 24a, no. 22.

Tomas, A., and Guittard, M. (1977) Une structure derivée de celle du spinelle: La structure de $Fe_{0.76}Yb_{2.16}S_4$. Materials Research Bulletin, 12, 1043–1046.

Vaughan, D.J., and Craig, J.R. (1978) Mineral chemistry of metal sulfides. Cambridge University Press, Cambridge.

——— (1985) The crystal chemistry of iron-nickel thiospinels. American Mineralogist, 70, 1036–1043.

Vaughan, D.J., and Tossell, J.A. (1981) Electronic structure of thiospinel minerals: Results from MO calculations. American Mineralogist, 66, 1250–1253.

Vaughan, D.J., Burns, R.G., and Burns, V.M. (1971) Geochemistry and bonding of thiospinel minerals. Geochemica et Cosmochimica Acta, 35, 365–381.

Von Philipsborn, H. (1974) Zur Kristallchemie Von Sulfide und Selenid Spinellen. Fortschritte der Mineralogie, 51, 201–239.

Manuscript received April 6, 1989
Manuscript accepted December 8, 1989